Supplementary Fig. 1

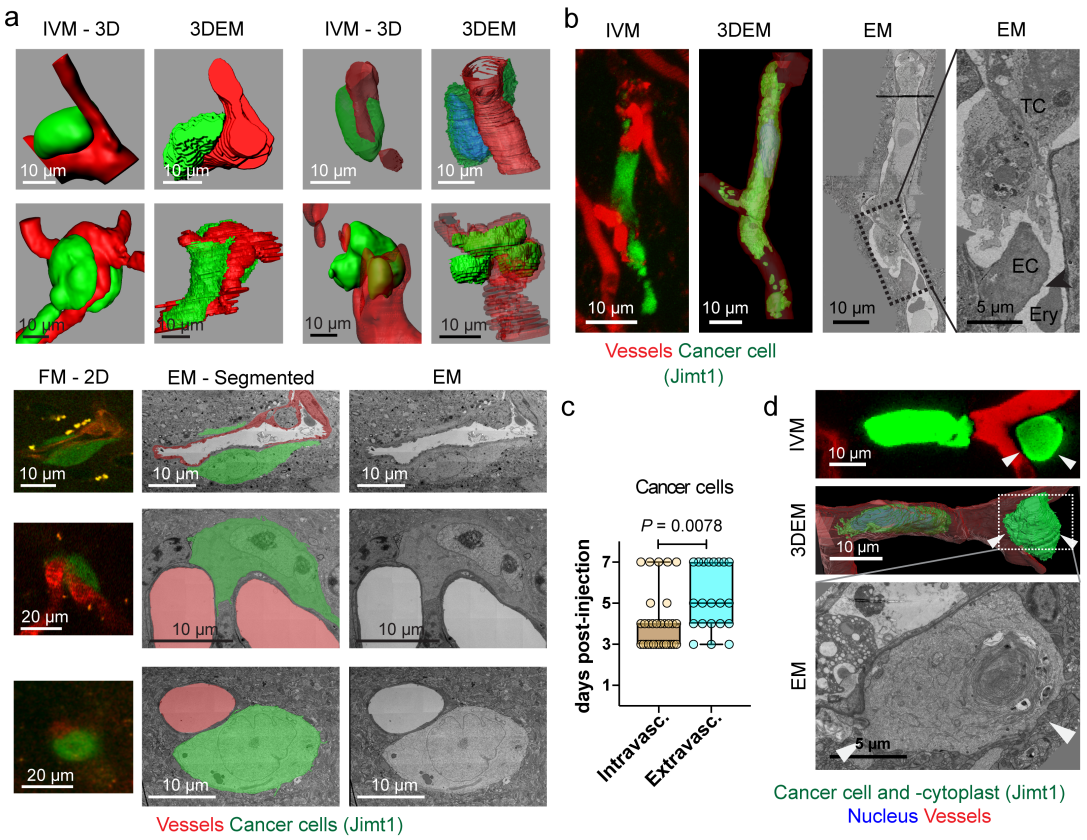

Supplementary Fig. 1: Earliest steps of metastatic brain colonization. a, Representative examples of extravascular Jimt-1 cancer cells (3-7 days p.i.) captured with multimodal correlative microscopy. IVM-3D: intravital microscopy 3D reconstruction, 3DEM: reconstruction from volume EM imaging, FM-2D: 2D sections from fluorescence microscopy, EM - Segmented: representative pseudo-colored EM section, EM: EM section. **b**, Representive correlative intravital and EM images of a Jimt-1 cancer cell (3 days p.i.) **c**, Quantification of intravascular and extravascular Jimt-1 cancer cells and associated cytoplasts found at 3, 4, 5 and 7 days p.i. (N=9 mice). *P* values determined by unpaired two-tailed t-tests with Welch's correction. **d**, as in b, but with extravascular cytoplast (arrowheads).

Supplementary Fig. 2

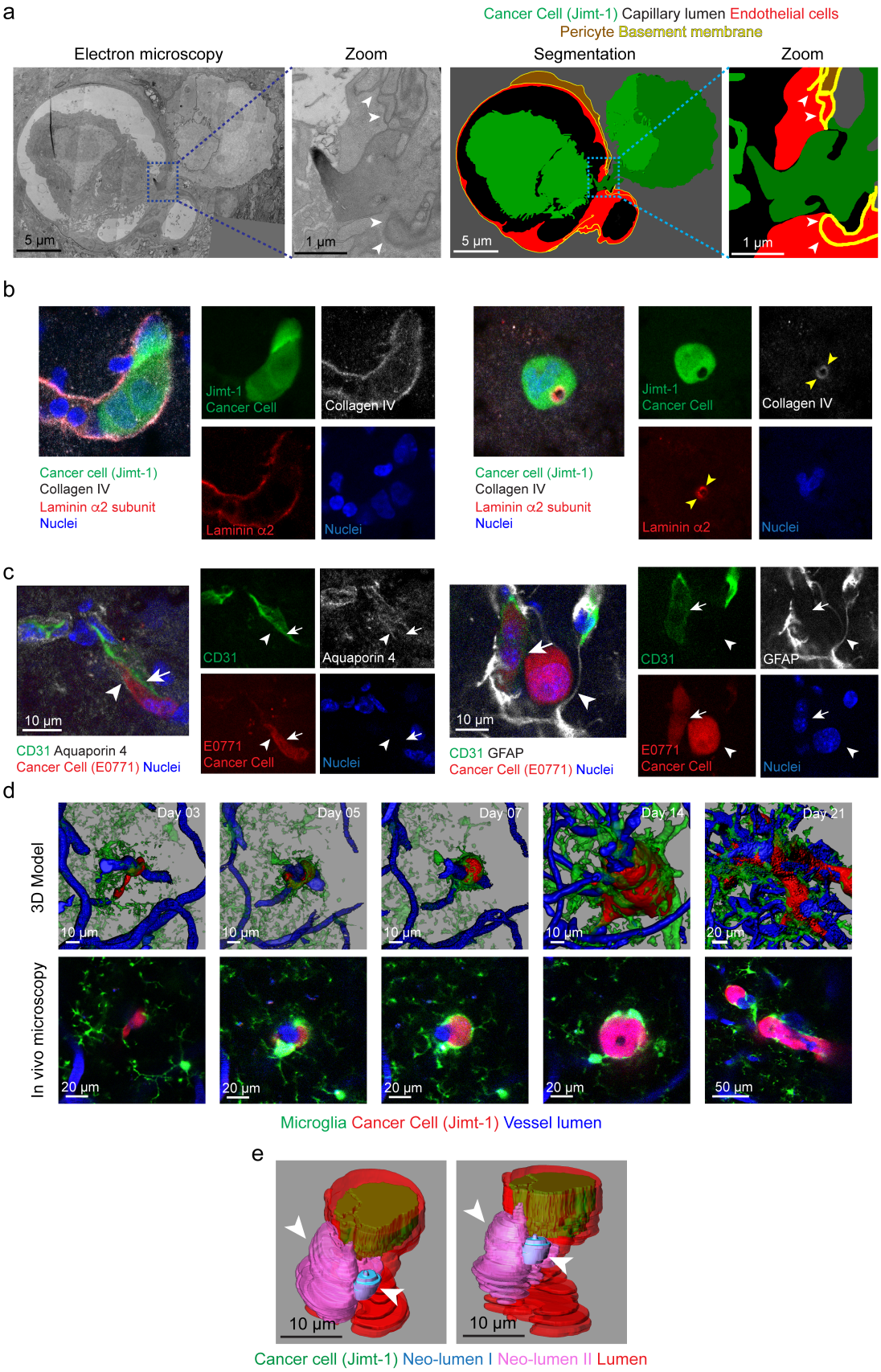

Supplementary Fig. 2: The neurovascular unit during cancer cell extravasation. a, Electron microscopy (left panels) of Jimt-1 cancer cell of which a small part is trans-endothelial, i.e. present both in the lumen and brain parenchyme (zoom). A fully intravascular Jimt-1 cell is also visible. The right panels show segmentation of ECs, the cancer cells, and the basement membrane (arrowheads). Note that the basement membrane is discontinued at the point where the cancer cell is crossing the blood brain barrier. **b**, Immuno histological staining of collagen IV, a component of the basement membrane, and laminin alpha-2, which is secreted specifically by astrocytes or pericytes into the basement membrane. At the level of the microcapillary, the endothelial and the astrocytic basement membrane are merged. Note that the both basement membrane components are perivascular to the extravasated cancer cell (right panels, arrowheads). **b**, Immuno histological staining of Aquaporin 4 (gray levels, left panels) and GFAP (gray levels, right panels) indicating the position of astrocytic endfeet and activated astrocytes, respectively, with respect to extravasated E0771 cancer cells (3 days p.i.). **b**, intravital microscopy of Jimt-1 intracardiacally injected in CX3CR1-GFP transgenic mice. Microglia are show in green, Jimt-1 in red and the vessel lumen in blue. Intravital microscopy (top panels: 3D models of the acquired z-stacks, bottom panels: single z-frames) enables to dynamically track the position of the microglia with respect to the developing BM over weeks. **c**, 3DEM reconstruction of part of a microvessel lumen (red) adjacent to an arrested Jimt-1 cancer cell (green, only shown in part, 7 days p.i.). In magenta and blue, two separated lumen are highlighted that are closed off from the main vessel lumen.

Supplementary Fig. 3

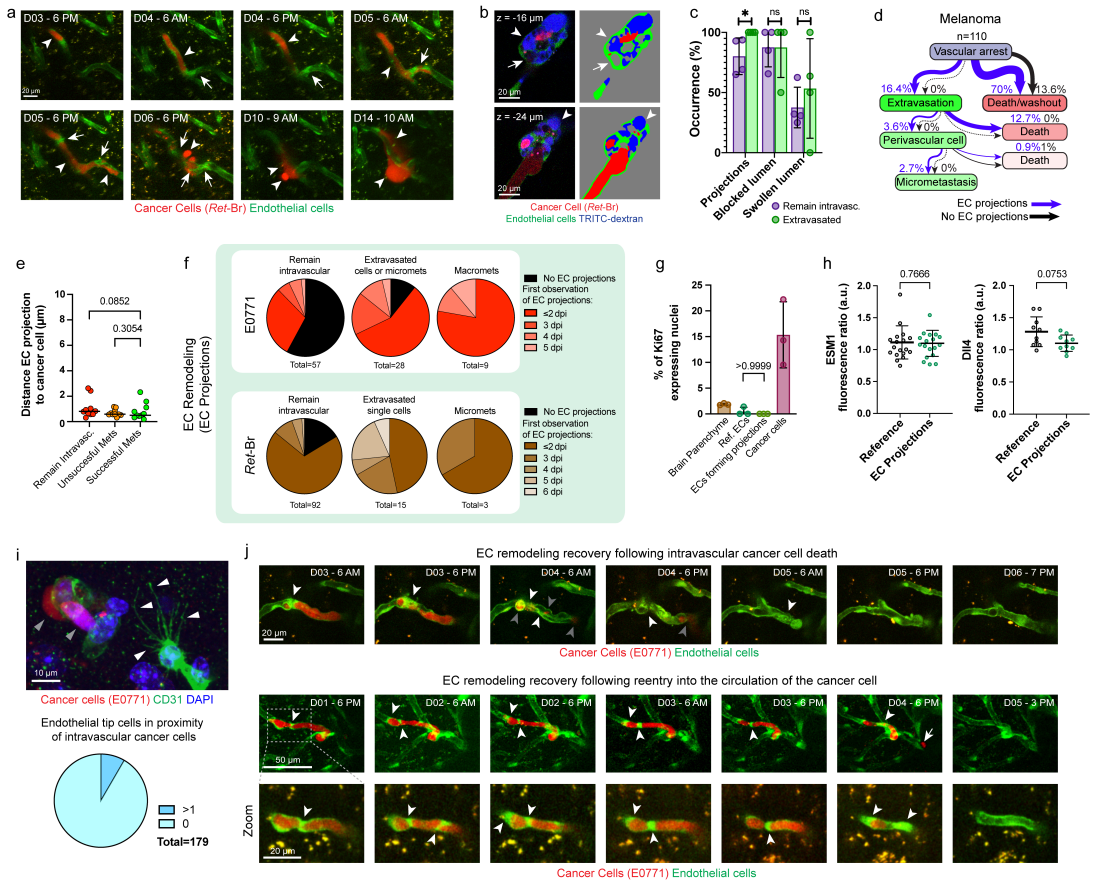

Supplementary Fig. 3: Intravital imaging of endothelial remodeling during metastatic brain colonization. a, Successful extravasation of a murine melanoma cancer cell (*Ret*-Br, red) shown here from day 3 p.i., 6:00 PM (D03) to the formation of micrometastasis (day 14 p.i., D14). High-frequency IVM enables capturing structural changes to both the cancer cell (arrowheads) and the ECs (green, arrows) surrounding it. **b,** EC Projections form separated compartments inside the capillary lumen where a *Ret*-Br cancer cell is trapped. Injection with an intravascular fluorescent dye reveals that these compartments are partly unperfused (arrow) with TRITC-conjugated to 500kD-dextran. Arrowhead indicates perfused region. **c**, Percentages of total *Ret*-Br cells remaining intravascular (Remain intravasc., purple) vs. total cells that extravasate (Extravasated, green) showing specific EC remodeling events (Projections, Blocked Lumen, Swollen lumen) in their direct proximity before or during extravasation (n=111 *Ret*-Br cells from 4 mice, quantification from IVM datasets). Data are mean ± s.d. *P* values determined by a Mann-Whitney test (*P* = 0.0286 for *). **d**, Quantification of the fate of distinct cancer cells (n=110 *Ret*-Br cells from 3 mice) as tracked over 14 days.

Cancer cells that are accompanied with EC projections, during arrest or extravasation, are indicated with blue arrows and percentages, and those cancer cells adjacent to which no EC projections were formed are indicated in black. **e,** Minimum distances of projections to intravascular E0771 cancer cells. Distance was measured from the closest projection to the cancer cell, for different outcomes; cell fails to extravasate ("remain intravasc."), cell extravasates but perishes in the perivascular niche ("unsuccesful mets"), or the cancer cell grows into a macometastasis ("succesful mets"). **f**, First IVM observations (days p.i., dpi) of EC remodeling (EC projections at the position of cancer cells that do not manage to extravasate ("remain intravascular"), those that extravasate but do grow further ("extravasated cells or micromets"/"Extravasated single cells") and those that continue growing ("Macromets" or "Micromets"). E0771 and *Ret*-Br cancer cells from N=3 mice per entity. **g**, Percentages of cells in the brain parenchyma (n=1990), endothelial cells (Ref: 203, peritumoral: 116) and E0771 cancer cells (n=46) expressing Ki67 (3 days p.i., from N=3 mice). **g**, Quantification of ESM1 and Dll4 expression in reference or EC-projections-forming EC at arrested E0771 cancer cells (3 days p.i., 18 positions from 3 mice (ESM1) and 10 positions from 1 mouse (Dll4)). *P* values were determined with a Mann-Whitney test. **h,** Fluorescence microscopy and quantification (bottom panel) of tip cell-like structures (white arrowheads) in microvessels in the proximity of E0771 cells (grey arrowheads), day 2 and 4 p.i., n=178 positions from N=6 mice. At 8.4% of the E0771 cancer cells, endothelial tip-cell-like structures were observed in neighboring vessels. **i**, IVM showing EC remodeling (arrowheads) at the site of an arrested E0771 cell followed by full recovery of the vessel after the cancer cell dies (top panels, grey arrowheads point to apoptotic fragments) or re-enters the circulation (white arrowhead shows moved part of cell). Bottom most panels depict the boxed area and show the EC remodeling (white arrowheads) at higher magnification.

Supplementary Fig. 4

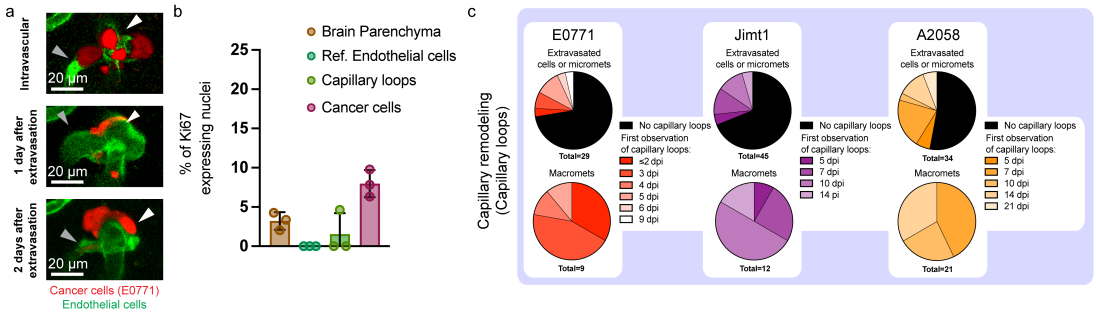

Supplementary Fig. 4: EC remodeling and vascular remodeling occurs at different time points during the metastatic cascade and are associated with successful growth.

a, IVM reveals early capillary loop formation following extravasation of an E0771 cancer cell. **b**, Percentages of cells in the brain parenchyma (n= 1378), of normal ECs (81), of ECs in capillary loops (n=163) and of E0771 cancer cells (n=1113) expressing Ki67 (ex vivo, day 14 p.i., from N=3 mice). **c** First IVM observations (days p.i., dpi) of vascular remodeling (capillary loop formation) at the position of cancer cells that only extravasate or show limited growth ("extravasated cells or micromets") and those that continue growing ("Macromets" or "Micromets"). E0771, Jimt-1 and A2058 from N=3 mice per model, data from IVM.

Supplementary Fig. 5

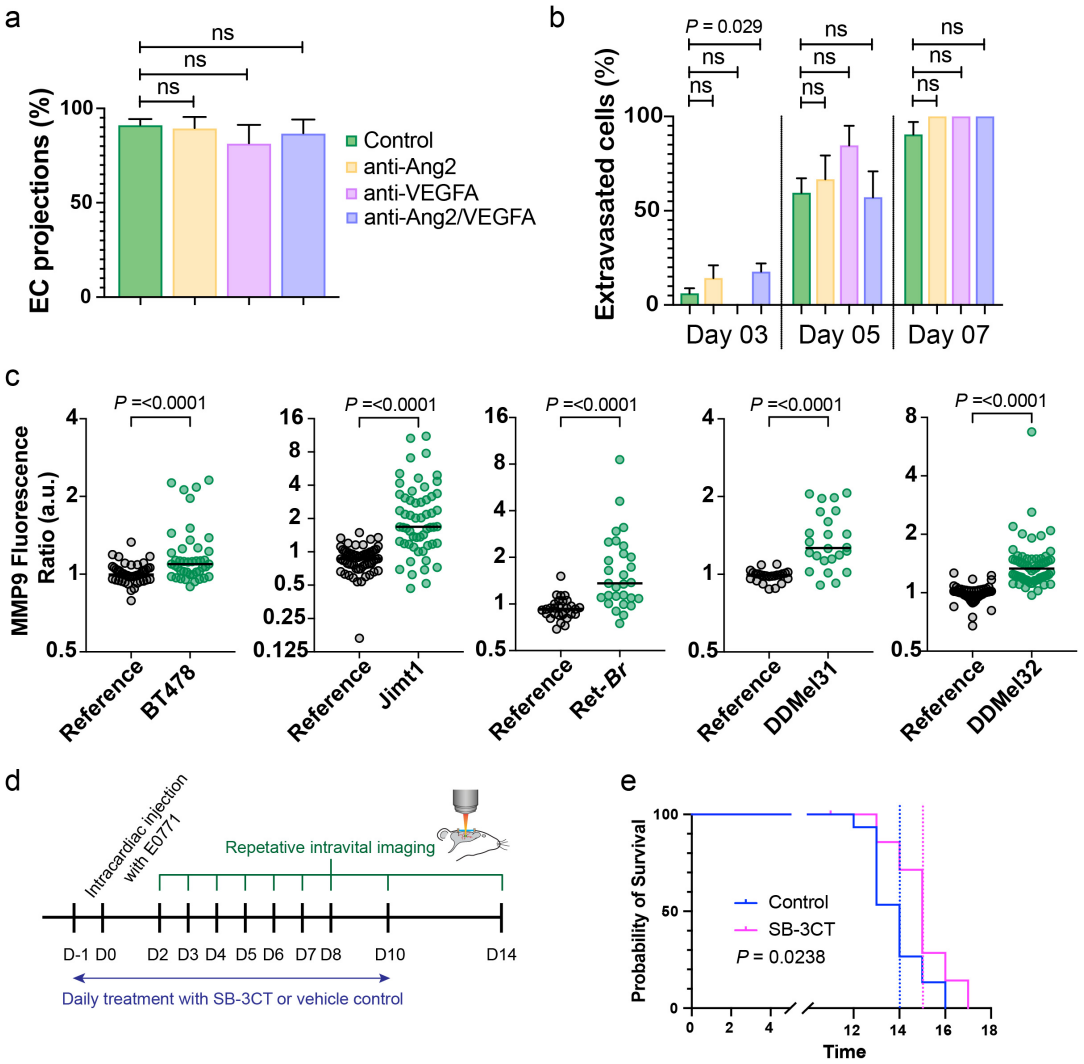

Supplementary Fig. 5: a, Quantification of EC projections formed in proximity of arrested cancer cells (16-42 intravascular cancer cells (*Ret*-Br) per treatment, from 3-4 mice) in mice treated with a control antibody vs. treatment anti-Ang2, anti-VEGFA or anti-Ang2/VEGFA antibodies. Data are mean ± s.e.m. *P* values are determined by Mann-Whitney test. **b**, Extravasation rate of cancer cells in control mice vs. mice treated with anti-Ang2, anti-VEGFA or anti-Ang2/VEGFA antibodies on day 3, 5 and 7 post intracardiac injection. (n=11-81 cancer cells (*Ret*-Br) per timepoint/treatment from 2-3 mice). *P* values are determined by Fischer's exact tests. **c,** Quantification of MMP9 at site of arrested cancer cells versus control vessels (Reference). .BT478 (primary cells from brain metastatic lung cancer), 4 days post-intracardiac injection, n=43 cells from N=3 mice, Wilcoxon Test. Jimt-1 (human breast cancer), 3-4 days post-intracardiac injection, n=56 from N=3 mice. DDMel31 (primary cells

from brain-metastic melanoma), 3-4 days post-intracardiac injection, n=24 cells from N=3 mice. DDMel32 (primary cells from brain-metastic melanoma), 4 days post-intracardiac injection, n=62 cells from N=3 mice. *P* values are determined by Mann-Whitney test. **d,** Schedule of control and SB-3CT treated mice, starting one day before intracardiac injection and continued up to day 10 p.i.. Mice are repetitively imaged during the course of the treatment to monitor the fate of each cancer cell. The experiment is terminated at day 14. **e,** Effect of MMP2/9 inhibition (starting 1 day before intracardiac injection until 10 days p.i.) with SB-3CT vs control treatment on overall survival of the mice intracardiacally injected with E0771. n= 14 vs n=15 mice per group in the SB-3CT and control group respectively. *P* value determined using a log-rank Mantel-Cox test.

Supplementary Fig. 6

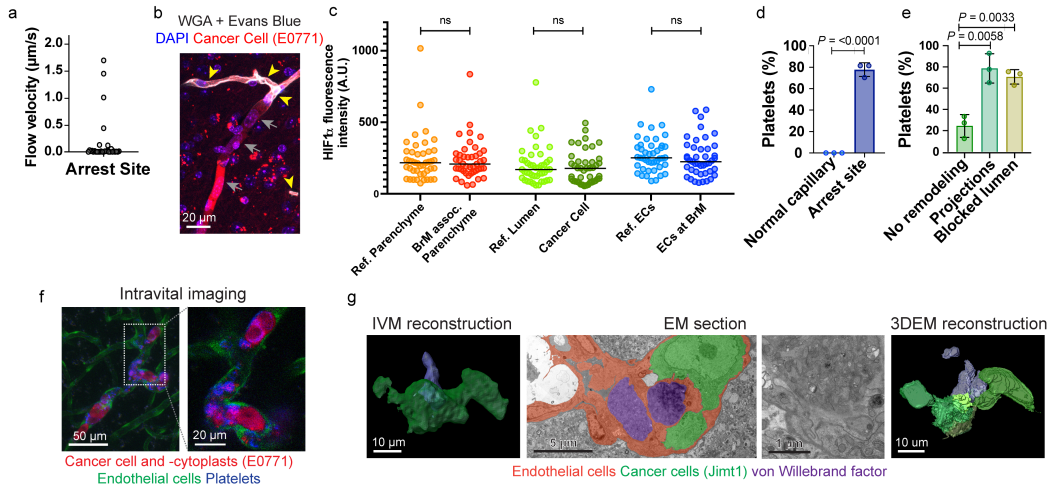

Supplementary Fig. 6: Reduced flow and clot formation at arrested cancer cells. a, Reduced or completely halted corpuscular capillary flow at the site of arrested E0771 cancer cell (red, day 6 p.i., shown in Fig. 6a). **b**, Arrested E0771 cancer cells (3 days p.i., gray arrowheads) blocks access of WGA + Evans blue dye to endothelial cells, whereas in perfused vessels the endothelial cells have taken up the dye (shown in white, highlighted by yellow arrowheads). **c**, Fluorescence intensity of HIF1α staining in the brain parenchyma, vessel lumen, and endothelial cells in the direct proximity of an arrested cancer cell (E0771, 3 days p.i.) or in reference areas. Data show medians, *P* values are determined by Wilcoxon tests. **d**, Quantification of percentage of intravascular cancer cells with intravascular platelet accumulation *in vivo* (77.78% ± 3.704) vs. control empty microcapillaries (reference, 0%±0) based on *in vivo* Rhodamin 6G measurements (81 E0771 cancer cells analyzed from 3 mice), data are mean ± s.d., *P* value is determined by an unpaired two-tailed t-test. **e,** Platelet accumulation at arrested cancer cells with respect to EC remodeling. Only in 24.4%±10.7 of arrest sites where no EC remodeling is found, platelets accumulate. At 78.6%±13.8 vs. 70.6%±6.9 of sites with EC projections or blocked lumen respectively, intravascular platelet accumulations are found *in vivo* (63 E0771 cancer cells from n=3 mice). Data are mean ± s.d., *P* values are determined by an unpaired two-tailed t-test **f**, IVM of platelet accumulation at intravascular arrested E0771 cancer cell with Rhodamin 6G (5 days p.i.). **g**, Multimodal correlative microscopy reveals accumulation of vWF-positive clots at arrested Jimt-1 cancer cells, 4 days p.i.. Injection of a fluororescently-conjugated anti-vWF antibody enables

visualization of vWF using intravital microscopy. By correlative microscopy, this fluorescent signal was found to co-localize to fibrillar clots accumulating inside the occluded lumen and cancer cell.

Supplementary Fig. 7

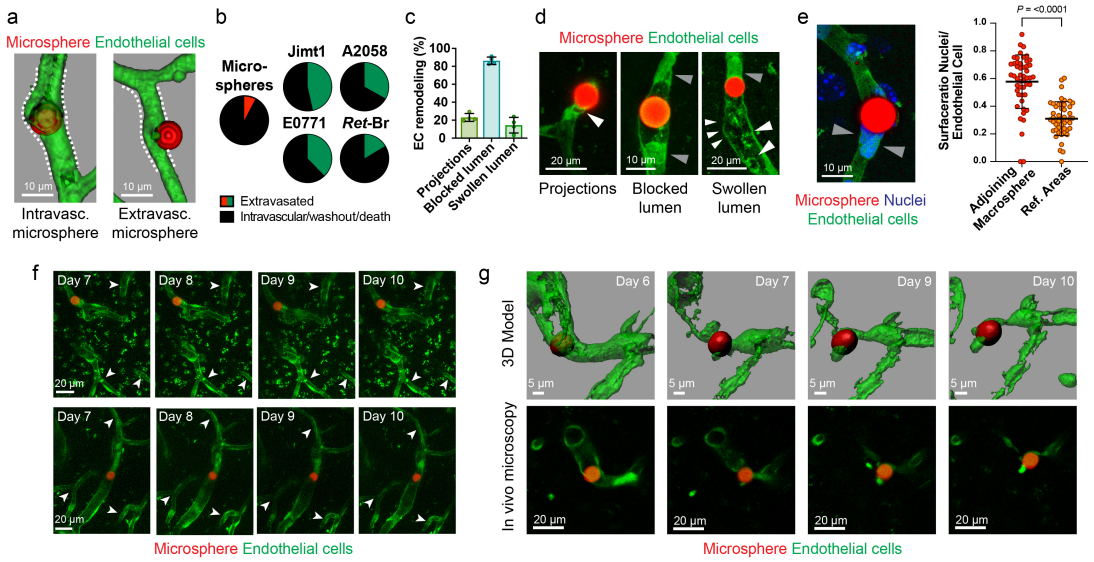

Supplementary Fig. 7: Extravasation of intracardiacally injected microspheres. a, Intracardiacally injected microspheres are intravascular and extravasated from the brain microcapillaries. Reconstructions of 3D fluorescence microscopy images, 10 days p.i.. **b**, Partition of microspheres (red) or cancer cells (green) that extravasate vs. their counterparts that do not (black) (Microspheres: n=52 microspheres from 3 mice (Extravasated: 7.7% vs. 92.3% Intravascular), Jimt-1: 112 cancer cells from 4 mice (Extravasated: 46.4% vs. 53.6% washout/death), A2058: 160 cancer cells from 3 mice (Extravasated: 33.1% vs. 66.9% washout/death), E0771: 106 cancer cells from 3 mice (Extravasated: 37.7% vs. 62.3% washout/death), *Ret*-Br: 110 cells from 4 mice (Extravasated: 16.4% vs. 83.6% washout/death)) **c-d**, Remodeling phenotypes adjacent to intravascularely arrested microspheres. 352 Microspheres from 4 mice, data are mean ± s.d. **e**, Endothelial cell nuclei block the capillary lumen adjacent to arrested microspheres. Right panel: Ratio of EC nuclei surface area over surface area of the partition of EC blocking the capillary lumen. 49 microspheres from 3 mice, data are mean ± s.d., *P* value is determined with a Mann-Whitney test. **f,** Intravital microscopy shows no angiogenesis or EC remodeling in capillaries (arrowheads) surrounding arrested microsphere. **g,** Intravital microscopy of intracardiacally injected microspheres reveals pruning of a microcapillary following microsphere arrest.

Supplementary Fig. 8

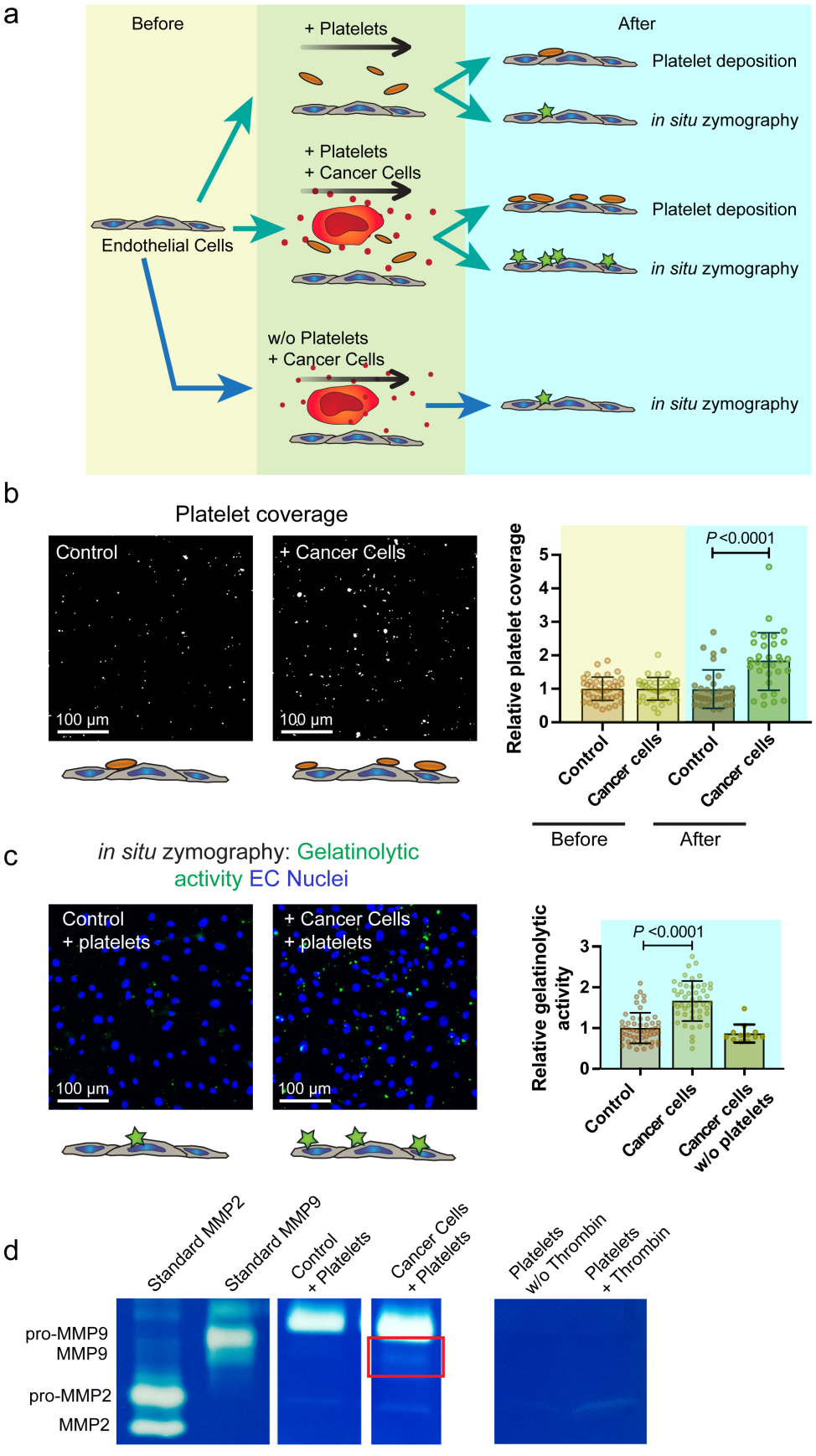

Supplementary Fig. 8: Activated platelets induce EC-mediated MMP9 excretion and activity *in vitro*. **a**, Schematic overview of the *in vitro* perfusion assay and subsequent quantification of platelet deposition and MMP activity by zymography. Unidirectional shear stress was applied using an IBIDI pump system to a monolayer of brain ECs. Fluorescent platelets were added to the system, in combination with cancer cells, to induce platelet activation, or without as a control. The impact of circulating murine melanoma cancer cells on platelet adhesion and gelanolytic activity was analyzed. **b**, Platelet coverage before and after incubation with additives was quantified per field. Data are normalized to platelet adhesion before incubation with additives (before) and presented as mean ± SD. **c**, After the *in vitro* perfusion assay, an in situ zymography was performed (**right**). Ibidi-slides were incubated with gelatin-FITC substrate (green) for 2 h and nuclei were co-stained with DAPI (blue). Quantification revealed a 1.7-fold increase in the gelatinolytic activity on the endothelial surface. **d**, After the microfluidic experiment, the activity of MMPs was analyzed in the supernatant by gelatin zymography. An increase of activated MMP9 after addition of cancer cells could be observed (red box). Platelets secrete only trace amounts of MMPs after activation by thrombin. A second band corresponding to latent proMMP2 enzyme was detected in all groups and remained unchanged.

Supplementary Fig. 9

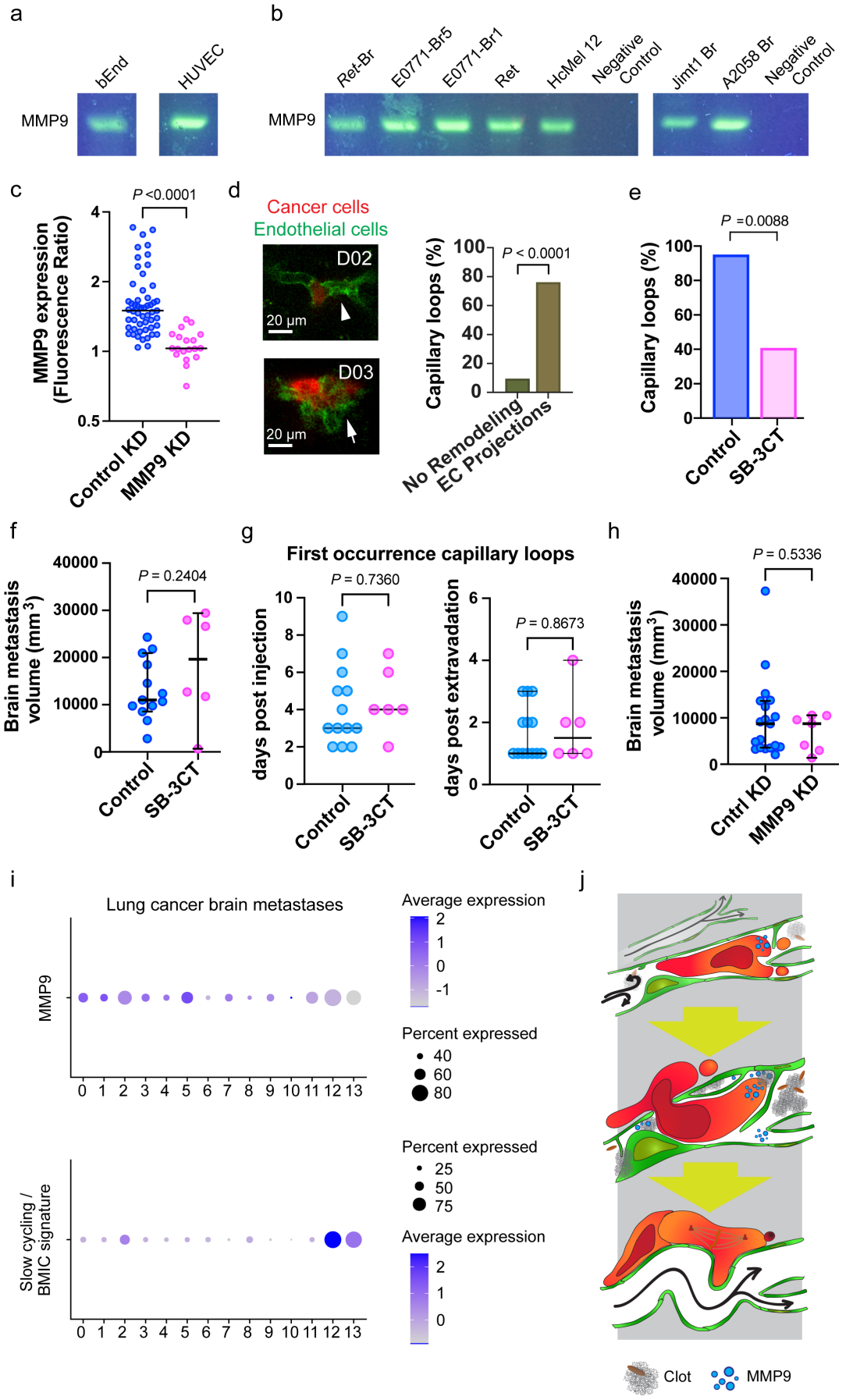

Supplementary Fig. 9: Expression of MMP9 and its effect on vascular remodeling *in vivo*. **a**,**b**, Expression of MMP9 was detected in murine and human and murine endothelial cells (a) and different cancer cell lines (b). All cell lines express MMP9 *in vitro*. **c**, MMP9 expression at the site of E0771 control KD and MMP9 KD cancer cells (n=53 control KD vs. 19 MMP9 KD E0771 cancer cells from 12 mice, 2 and 4 days p.i.). *P* values were determined by a Mann-Whitney test. **d**, Intravital imaging shows that EC projections precede capillary loops formation at the same site. Graph: quantification of capillary loops formed at positions where the previous day no EC remodeling subtypes were observed ("No EC Remodeling") or where EC projections were present. (n= 21 extravasated E0771 cancer cells from 3 mice, *P* values determined by Fischer's exact test). **e**, Quantification of capillary loops formed at the position of extravasated E0771 cancer cells in control (92.86% of n=14 cells from 3 mice) and SB-3CT (40% of n= 10 cells from 3 mice) treated mice. *P* values determined by a Fischer's exact test. **f**, Volumes of E0771 metastases at which capillary loops were found, in control or SB-3CT treated mice (IVM, day 2-14 p.i.). Volumes were measured at the earliest timepoint when capillary loops were observed (Control: n=13 metastases from 3 mice, SB-3CT: n=6 metastases from 3 mice). *P* values were determined by an unpaired t-test. Data are median with 95% CI **g**, first observation made with IVM of capillary loops accompanying E0771 metastases in control or SB-3CT treated mice. Left panel: days following intracardiac injection, right: days following extravasation. **h**, Volumes of E0771 metastases at which capillary loops were found in metastases from control KD and MMP9 KD E0771 cancer cells (immunohistofluorescence staining, 4 days p.i., n=19 control KD cells from 4 mice vs. n=7 MMP9 KD cells from 4 mice). *P* values were determined by a Mann-Whitney test. Data are median with 95% CI. **i**, Dot plots of expression of MMP9 (top panels) and genes associated with slow-cycling, BMIC cells[1] (bottom panels) in different clusters of lung cancer brain metastatic cancer cells. Data was obtained *in silico* from single cell RNA sequencing data from 3 BM of both entities[2]. **j**, Schematic illustration of tumor cell extravasation from the brain microcapillary. The left of the scheme depicts an arrested cancer cell with blocked flow of blood cells (arrows) and to the left a non-pathological capillary. In the middle, extravasation of a cancer cell is shown including clots, MMP9 activity and endothelial remodeling. To the right, early perivascular growth is shown including capillary loops.

Supplementary Movies

Supplementary Movie 1: 3D Electron microscopy of a Jimt-1 cancer cell arrested in a brain microcapillary. A 3D model of the cancer cell, its nucleus and the surrounding vasculature is shown, followed by a zoom of the EM dataset.

Supplementary Movie 2: 3D models of an extravasating Jimt-1 cancer cell (green) captured with intravital correlative microscopy. Capillaries are shown in red. The 3D model of the IVM dataset is shown above, from the 3DEM dataset below. The extravasation event is highlighted with the yellow box, and is shown in detail in Supplementary Movie 3.

Supplementary Movie 3: 3D EM of an extravasation event of an Jimt-1 cells captured with intravital correlative microscopy (Supplementary Movie 2). Top panels show the EM z-stack, acquired from serial sections, bottom panels the segmentation of the Jimt-1 cancer cell and associated cytoplasts (shades of green), the cancer cell nucleus (blue), ECs (shades of red) and the basement membrane (yellow). Note the pathological remodeling for the basement membrane at the extravasation site.

Supplementary Movie 4: Intravital microscopy of arrest, extravasation and brain colonization of and E0771 cancer cell. White arrowheads point to remodeling events, the grey arrowhead to the extravasating cancer cell. Scale bar represents 20 µm.

Supplementary Movie 5: Intravital microscopy of an arrested and extravasating E0771 cancer cell (red) in the brain microcapillary of a *VE-Cad Cre^{ERT2}xRosa26-YFP$^{fl/fl}$* mouse (ECs shown in green). Flow of erythrocytes is visible (bottom panels) owing to intravascular injection of TRITC dye (blue in the left panels and top panels), white in the right bottom panels). Excessive swelling and EC projections are observed on D06, where the metastasis is part intravascular and part extravascular. Note that following extravasation of the E0771 cancer cell it perishes and disappears from view (Day 9, D09) The blocking of flow results in

temporary pruning of the microcapillary (arrowhead in D09 and D10), followed by its reopening on D13 (left arrowhead). A small, new lumen is also observed (right arrowhead, D13). On D14 the flow is fully restored.

Supplementary Movie 6: Intravital microscopy of a growing metastasis from E0771 cancer cells (red) and associated vasculature (blue) from day 3 to day 14. Yellow arrowheads point towards capillary loops.

Supplementary Data: Materials and Methods

In vivo microscopy of brain metastases-associated microglia

To visualize microglia in a xenograft model of breast cancer brain metastases (Jimt-1 expressing tdTomato), B6.129P-Cx3cr1tm1Litt/J[3] (JAX stock #005582,) were crossed with Foxn1nu to generate B6.129P-Cx3cr1tm1Litt/J x Foxn1nu. For these experiments we used CX3CR1$^{+/GFP}$ animals, expressing both GFP and functional CX3CR1 [3,4]. Mice weighing at least 20g were implanted a cranial window and following minimally three weeks of recovery, Jimt-1 tdTomato cells were intracardially injected. Intravital imaging was performed over a period of 4 weeks p.i. to follow the growth of each brain metastases and their interaction with the fluorescent microglia.

Image analyses

The distance of EC projections to the cancer cell was measured from intravital imaging datasets (E0771 in VE-Cad mice). Hereto, we selected 10 datasets each of cancer cells that form successful metastases, extravasate or remain intravascular. The EC projection closest to the cancer cell was selected and in a single z-plane this distance was measured using Fiji[5]. Quantification of expression of Ki67 was performed by counting the number of nuclei fluorescently labelled positively for Ki67 divided by the total number of nuclei in each compartment.

PDX Models

The patient-derived cell lines DDMel31 (BRAF-V600E-, NRASQ61+) and DDMel32 (BRAF-V600E-, NRASQ61R+) were isolated from human melanoma BM (Dresden, Germany). In order to exclude the possibility of establishing tumor associated fibroblasts, the primary cell lines were tested for their NRAS or BRAF mutation status and for their expression of the melanoma markers Melan A, tyrosinase and HMB45. The cells were cultured in RPMI medium with 10% fetal bovine serum, 1% penicillin-streptomycin-amphotericin B and 1% L-glutamine. The patient-derived cell line BT478 (a kind gift from Sheila Singh) was cultured as described before[6]. To study expression of MMP9, the patient-derived cell lines were injected in NOD-*scid IL2rγ*^{null} (NSG, initially generated by Jackson Laboratory) and the mice were

sacrificed 3-4 days p.i. by perfusion fixation. Vibratome or cryosections of the mouse brains were stained for MMP9 and CD31 as described in the Materials section of the main text.

Survival experiment

Mice were treated with SB-3CT (n=15 mice) or control (carrier solution, n=14 mice), as described in the main text, from one day before intracardiac injection with E0771 until 10 days p.i.. Clinical scoring was performed daily, and mice were euthanized as soon as humane endpoint was reached.

WGA and Evans Blue staining

To allow histological visualization of the vessels, as described before[7], 150 µL of 2% Evans Blue (E2129-10G, Sigma-Aldrich, USA) in sterile PBS was injected intraperitoneally 12 hours prior to perfusion of the mice. For perfusion, 15 mL of PBS and 150 µL of WGA-Alexa 633 (5mg/mL, W21404, Thermo Fischer Scientific, USA) is first injected intracardially, followed by 15 mL of 4.5% PFA (Roti-Histofix 4.5%, 2213, Carl Roth, Germany). After perfusion, the brain was harvested and used for histological studies.

In vivo microscopy of platelets and von Willebrand Factor (vWF)

To visualize platelets by intravital imaging, Rhodamine 6G dye (0.1 mL, 0.5 mg/mL in 0.9% NaCl, R4127-5G, Sigma-Aldrich, USA) was intravenously injected into the tail vein of the mouse shortly before imaging and visualized at 850 nm as described above. Clot formation was defined as a visible intravascular cluster of platelets. A FITC-conjugated anti-von Willebrand Factor antibody (GTX28822, GeneTex Inc., USA, RRID:AB_369684) was used to visualize vWF *in vivo*. Purification of the antibodies for *in vivo* use was performed via a desalting column (HiTrap, GE29-0486-84, Sigma-Aldrich, USA). Prior to imaging, 3.5 µg g^{-1} body weight of antibody dissolved in 0.2 mL PBS was injected into the tail vein of the mouse. VWF accumulation was semi-quantitatively identified as a >150% local increase in FITC intensity in contrast to the background intravascular signal.

VEGFA, Ang2 and VEGFA/Ang2 inhibition *in vivo*

Eight to 12 weeks old C57BL/6 mice were treated with control (MOPC21), anti-Ang2 (LC06, RO6872894), anti-VEGFA (B20.4.1, RO6872895), or anti-Ang2/VEGFA antibodies

(LC06/B20.4.1, RO6872840) (F. Hoffmann-La Roche, Penzberg, Germany) as described before[8]. The antibodies were administered in a concentration of 5 mg/kg body weight in NaCl administered into via intraperitoneal injection every third day starting from one day before heart injection. For this experiment, *Ret*-Br cells were intracardiacally injected as described above. To determine endothelial remodeling before, during and after extravasation, the mice were perfusion fixed at day 3, 5 or 7 following intracardiac injection of cancer cells, and brain sections were processed and stained for CD31/PECAM-1 as described in the materials and methods of the main text. Cryosections or 100 µm vibratome sections of the fixed brains were stained for CD31 and imaged with and LSM 710 or 780 (Zeiss, Germany). Endothelial remodeling and cancer cell position with respect to the vessel was scored.

Cell culture for *in vitro* perfusion assay and zymography

The murine brain endothelial cell line (bEnd.3; ATCC Genuine Cultures® CRL-2299™, USA, RRID:CVCL_0170) was grown in a 0.5% Gelatin coated surface in Dulbecco's Modified Eagle's Medium (DMEM) (Merck) supplemented with 10% FBS. A murine melanoma cell line, isolated from *Ret* transgenic mice, was maintained in RPMI-medium supplemented with 10% heat-inactivated fetal calf serum (FCS), 1% non-essential amino acids, 1% glutamic acid and 1% pen/strep. The incubation was performed at 37°C in a humid atmosphere of 5% carbon dioxide.

Isolation of platelets

Platelets were isolated from citrated blood of human volunteers according to the approval of the local ethics committee. After centrifugation (120 g, 15 minutes), the platelet-rich plasma was transferred into washing buffer (103 mM NaCl, 5 mM KCl, 3 mM NaH_2PO_4* H_20, 5 mM HEPES, 5.5 mM Glucose) with a pH of 6.5 and 1 U/ml of Apyrase (Sigma-Aldrich), centrifuged (1200 g, 15 minutes) and washed.

***In vitro* perfusion assay**

bEnd.3 cultured on a μ-Slide $I^{0.2}$ Luer IBIDI-slide (IBIDI GmbH, Munich, Germany) were perfused at 2.5 dyne/cm² with isolated platelets and a hematocrit of 25% in HEPES-buffered saline using the IBIDI air pressure pump system. Platelets were labeled using Celltrace TM Orange AM (1:1000; Invitrogen, Germany). First, ECs were superfused for 5 min with or

without isolated platelets without addition of stimuli. Next, ECs were stimulated with Ret cells (500.000/ml) or medium without additives and perfused for 15 min. Analysis was performed using a Zeiss AxioObserver Z1 equipped with an AxioCam MRc (Carl Zeiss AG, Oberkochen, Germany).

***In situ* zymography**

In situ gelatinolytic activity was analyzed using a commercially available kit (Molecular Probes, Germany). μ-Slide $I^{0.2}$ Luer IBIDI-slide were incubated for 2h at 37 °C in a reaction buffer containing the gelatin fluorescein conjugate (50mg/mL) without washing. After fixation with ice-cold acetone for 30s nuclei were stained with DAPI (1:5000 in PBS) for 10 mins and the microscopic analysis was performed using a Zeiss AxioObserver Z1 equipped with an AxioCam MRc (Carl Zeiss GmbH, Germany).

Gel zymograpy

Gel zymography was performed as described[9] with some modifications. After the in vitro perfusion assays, the supernatant of μ-Slide $I^{0.2}$ Luer IBIDI-slides was collected. Equal amounts of samples were electrophoretically separated on 8.0% SDS-PAGE gels co-polymerized with 2mg/mL gelatin (Sigma) under non-reducing conditions. Gels were incubated in washing buffer containing 2.5% Triton X-100 and then incubated for 40 h in developing buffer (50 mmol/LTris/HCl, 10 mmol/L CaCl2, 0.02% NaN3) at 37 °C before staining with Coomassie blue R-250 (250mL Methanol, 35mL acetic acid, 1.25 g Brilliant Blue) for 1 h. Gels were destained in 5% acetic acid and 25% methanol until clear bands manifesting gelatinolysis appeared on the blue background. Quantification was performed using ImageJ.

RT - PCR

RNA from bEnd.3, HUVEC and the different tumor cell lines was isolated using the RNeasy Mini Kit (Qiagen, Germany) according to the manufacturer's protocol. The cDNA was synthesized from 1 µg of total RNA per sample using the Maxima First Strand cDNA Synthesis Kit (Thermo Fisher Scientific, USA). To detect the mRNA transcript from cDNA, polymerase chain reaction (PCR) was performed using the GoTag G2 DNA Polymerase (Promega, Germany) and specific primers to human and mouse MMP9. Primers used for

Mmp9 (mouse): Forward 5'- -3' GACATGATCGATGACGCCTTCG; Reverse: 5'- -3' CTTTGCCCAGCGACCACAAC. For MMP9 (human): Forward 5'- -3' CTACTCGGAAGACTTGCCGCG; Reverse: 5'- -3' ATCTGCGTTTCCAAACCGAGTTG.

References

1. Berghoff, A. S. *et al.* Identification and Characterization of Cancer Cells That Initiate Metastases to the Brain and Other Organs. *Mol Cancer Res* (2020). doi:10.1158/1541-7786.MCR-20-0863
2. Gonzalez, H. *et al.* Cellular architecture of human brain metastases. *Cell* **185,** 729–745.e20 (2022).
3. Jung, S. *et al.* Analysis of Fractalkine Receptor CX3CR1 Function byTargeted Deletion and Green Fluorescent ProteinReporter Gene Insertion. *MOLECULAR AND CELLULAR BIOLOGY* **20,** 4106–4114 (2000).
4. Feng, X. *et al.* Loss of CX3CR1 increases accumulation of inflammatory monocytes and promotes gliomagenesis. *Oncotarget* **6,** 15077–15094 (2015).
5. Schindelin, J. *et al.* Fiji: an open-source platform for biological-image analysis. *Nature Methods* **9,** 676–682 (2012).
6. Singh, M. *et al.* Therapeutic Targeting of the Premetastatic Stage in Human Lung-to-Brain Metastasis. *Cancer Research* **78,** 5124–5134 (2018).
7. Todorov, M. I. *et al.* Automated analysis of whole brain vasculature using machine learning. *bioRxiv* 613257 (2019). doi:10.1101/613257
8. Solecki, G. *et al.* Differential Effects of Ang-2/VEGF-A Inhibiting Antibodies in Combination with Radio- or Chemotherapy in Glioma. *Cancers* **11,** (2019).
9. Bauer, A. T., Bürgers, H. F., Rabie, T. & Marti, H. H. Matrix metalloproteinase-9 mediates hypoxia-induced vascular leakage in the brain via tight junction rearrangement. *J Cereb Blood Flow Metab* **30,** 837–848 (2010).